The Effect of the Spatial Sensitivity of TDR on Inferring Soil Hydraulic Properties from Water Content Measurements Made during the Advance of a Wetting Front

Ty P. A. Ferré,* Henrik H. Nissen, and Jirka Šimůnek

ABSTRACT

Many measurement methods are considered to return point values of volumetric water content, water pressure, or other hydrologically relevant properties. However, many methods have spatially distributed measurement sensitivities, averaging a property of interest over some sample volume. In this investigation, we study the effects of the spatially distributed measurement sensitivity of time domain reflectometry (TDR) on the inversion of hydraulic properties from water content measurements. Specifically, a numerical analysis of the water breakthrough curves that would be measured by TDR probes of varying designs during the advance of a wetting front is presented. Numerical inversion of these water breakthrough curves is performed to estimate the soil hydraulic parameters. Time domain reflectometry probes with larger rod separations show less impact on the flow of water at the wetting front. However, these probes have more widely distributed spatial sensitivities, leading to more smoothing of the observed water breakthrough curve. The TDR-measured wetting front shape is more distorted for vertically emplaced probes than for horizontal probes. The optimal TDR probe configuration for inversion of hydraulic parameters from measurements recorded during the advance of a vertical wetting front has three closely spaced rods that lie in a common horizontal plane. The inversion results using this design show close agreement with known values and very small 95% confidence intervals of the inverted properties. This specific recommendation cannot be adopted generally for all TDR monitoring applications. Rather, we recommend that a similar analysis be performed for each specific monitoring application. While the results presented are specific to TDR responses, the same consideration should be given to all instruments with spatially distributed sensitivities.

TIME DOMAIN REFLECTOMETRY has become a standard instrument for water content measurement since its introduction by Topp et al. (1980). Time domain reflectometry has been shown to give accurate water content measurements in a wide range of porous materials with little need for soil-specific calibration. In addition, the continual advance of TDR instrumentation and associated software has led to the ready availability of off-the-shelf TDR monitoring systems. Like other indirect water content measurement methods (e.g., neutron probes and capacitance probes), TDR measures some average water content in a volume of medium surrounding the probes. One unique aspect of TDR is the ease with which a user can alter the sample volume and spatial sensitivity of TDR probes. For the TDR method, this spatial sensitivity has been examined both analytically (Knight, 1992) and numerically (Knight et al., 1997). Further examination has shown the dependence of the TDR spatial sensitivity on the size and orientation of TDR probes (Ferré et al., 1998; Nissen et al., unpublished data). On the basis of these analyses, users can design probes for specific monitoring objectives (e.g., Nissen et al., 2002). For example, the number and relative position of the rods comprising the probe can be altered to achieve high-resolution measurements within small sample volumes adjacent to the rods or to return water content measurements that are representative of larger sample volumes farther from the rods. Despite these advances, there has been little consideration of the effects of this spatial sensitivity on the utility of TDR for monitoring hydrologic processes. Furthermore, the presence of the impermeable rods will have some effect on water flow. Therefore, an analysis of the mutual effects of the spatial distribution of dielectric permittivity, the spatial sensitivity of TDR probes, and the effects of TDR rods on water flow is necessary to choose the optimal probe design for any specific measurement application.

In this investigation, we study the optimal probe design to infer soil hydraulic properties from measurements made during the advance of a wetting front into initially dry sand. These conditions lead to a strong dielectric permittivity contrast across a sharp wetting front. Given that the spatial sensitivity of TDR probes depends upon the spatial distribution of dielectric permittivity, these are considered to be the most challenging conditions for representative water content measurement with TDR. We designed a numerical study to evaluate the effects of TDR probes and TDR spatial sensitivity on the numerical inversion of hydraulic properties. Initially, we used a numerical forward model of unsaturated water flow to simulate the advance of a wetting front past TDR rods of varying geometries. We then used a numerical analysis of the spatial sensitivity of TDR probes to predict the water content that would be measured as a function of time for different probe designs. Finally, we used numerical inversion of the TDR responses to estimate soil hydraulic properties, thereby identifying potential errors in hydraulic property inversion arising from TDR-measured water contents.

The objectives of this investigation are (i) to determine whether TDR probes cause significant disruption to flow during the advance of a wetting front, (ii) to determine whether numerical inversion of TDR-measured water contents leads to accurate estimates of soil hydraulic properties, and (iii) to determine whether any inversion errors that may result can be minimized by the correct choice of TDR probe design and orientation.

Ty P.A. Ferré, Department of Hydrology and Water Resources, University of Arizona, AZ; Henrik H. Nissen, Department of Environmental Engineering, Institute of Life Sciences, Aalborg University, Denmark; and Jirka Šimůnek, George E. Brown, Jr., Salinity Laboratory, USDA-ARS, Riverside, CA. Received 15 May 2002. *Corresponding author (ty@hwr.arizona.edu).

Abbreviations: TDR, time domain reflectometry.

Table 1. The values of α, n, and K_s used in the forward model (Actual), those determined through inversion of the water content at the center of the domain with no rods present as a function of time (No rods), those determined from the water content at the mid depth of the domain with 2H, 2V, and 3H TDR probes present (designated as "rods"), and those determined from inversion of the water contents measured with 2H, 2V, and 3H TDR probes.†

Scenario	α	n	K_s	R^2
	m^{-1}		m s^{-1} × 10^{-5}	
Actual	14.5	2.68	8.25	
No rods	14.4 (13.9–4.8)	2.70 (2.66–2.74)	8.13 (7.88–8.38)	>0.999
2H(0.01) rods	14.5 (14.0–15.0)	2.69 (2.62–2.77)	8.23 (7.87–8.58)	>0.999
2V(0.01) rods	15.1 (14.4–15.7)	2.67 (2.61–2.72)	8.46 (8.10–8.82)	>0.999
3H(0.01) rods	14.0 (13.0–15.0)	2.74 (2.60–2.87)	7.98 (7.36–8.60)	>0.999
2H(0.005) rods	13.9 (12.9–15.0)	2.75 (2.62–2.88)	7.92 (7.28–8.57)	>0.999
2H(0.01)	12.1 (9.08–15.0)	2.44 (2.15–2.73)	7.32 (5.18–9.46)	0.992
2V(0.01)	16.0 (12.2–19.8)	2.06 (1.83–2.29)	8.95 (6.85–11.1)	0.968
3H(0.01)	14.5 (13.0–16.1)	2.54 (2.38–2.69)	8.57 (7.53–9.60)	0.998
2H(0.005)	12.1 (10.2–13.9)	2.59 (2.38–2.80)	7.16 (5.81–8.51)	0.997

† The values shown in parentheses are the 95% confidence intervals of the parameter values as reported by HYDRUS-1D.

METHODS

HYDRUS-2D (Šimůnek et al., 1999) was used to simulate the vertical advance of a wetting front into a two-dimensional cross-section by numerically solving the Richards' equation. The soil hydraulic properties (Table 1) were chosen to represent those of sand based on the ROSETTA (Schaap et al., 2001) database. The simulation domain was 0.05 m wide and 0.05 m deep. Initially, the pressure head was a constant −0.5 m throughout the domain. (Note that all pressure heads are expressed as meters of water.) The lateral boundaries were no flux. The upper boundary was held to a constant pressure head of 0 m, representing ponded infiltration, and the lower boundary was held to a constant −0.5 m. The simulation time was 60 s. TDR probes were placed within the transport domain as impermeable objects and were represented as circular no flow boundaries. "Horizontal" probes were placed such that all of the horizontal rods were located in a common horizontal plane, while "vertical" probes had horizontal rods located in a common vertical plane (Fig. 1). All of the rods were placed such that the center of the TDR probe was located at the center of the domain. Probes were chosen to represent very small probes like those that may be used in column experiments. As such, the probes were comprised of 0.0015-m-diameter rods. For comparison of probe geometries, "Two-rod" probes were represented as two parallel rods with the centers of the rods separated by 0.01 m. "Three-rod" probes had three equally spaced rods, with the outermost two rod centers

Fig. 1. Finite element domain used to simulate the advance of a wetting front into a domain with an initial uniform pressure head of −0.5 m. The circular holes in the domain are no-flow boundaries to represent the obstruction to flow caused by a 2H(0.01) TDR probe. Schematic vertical cross-sections of 2V and 3H probes are shown as well. The rods lie in the horizontal plane for all of the probe designs.

separated by 0.01 m. To examine the effects of rod separation, further simulations were conducted for two-rod horizontal and vertical probes with separations of 0.005 and 0.02 m. The probes are described based on the number of rods, the orientation, and the separation of the outermost rods. For example, the two-rod horizontal probe with the rods separated by 0.01 m is referred to as the 2H(0.01) probe.

Nissen et al. (unpublished data) found that 3V probes can give rise to the simultaneous transmission of multiple waves traveling at different velocities if the dielectric permittivity varies between two adjacent rods. This precludes the application of travel time measurement to determine the volumetric water content. As a result, this probe design is not recommended for monitoring the advance of a wetting front. Therefore, we considered only 2H, 2V, and 3H probes.

An example of the finite element domain used to simulate water flow around a 2H(0.01) probe is shown on Fig. 1. An effort was made to make the finite element grid geometries used in all of the simulations as similar as possible. To achieve this, circles outlining all of the rods were included in all of the simulation domains. In total, 13 circles were used. Those circles that were not used to represent rods in any given simulation were filled with elements. Circles representing rods were impermeable holes in the grid. An observation point was placed at the midpoint of each probe, located at the center of the domain. Given that an observation point cannot be placed in the center of the domain for the three-rod probes, which have a rod centered at the domain center, the observation point for these probes was placed at a point equidistant from an outer and the inner rod.

The water content, θ (m³ m⁻³), distribution within the domain was determined every 2.4 s for 1 min of simulation time, for a total of 26 water content distributions. The relative dielectric permittivity, K, distribution was determined from the water content distribution based on the linear form of the Topp et al. (1980) relationship presented by Ferré et al. (1996):

$$K^{0.5} = 8.47\theta + 1.56 \qquad [1]$$

For each simulated time, the numerical analysis of Knight et al. (1997) was then used to determine the dielectric permittivity that would be measured for the given TDR rod distribution on the basis of the dielectric permittivity distribution at that time. This analysis is based on the determination of the spatial distribution of the energy of the electromagnetic field in the plane transverse to the direction of electromagnetic plane wave propagation. Knight (1992) showed that this distribution could be used to define the spatial sensitivity of a TDR probe in the transverse plane. We use the numerical analysis to determine the weighted average dielectric permittivity that would be measured by a TDR probe of a given configuration for a given
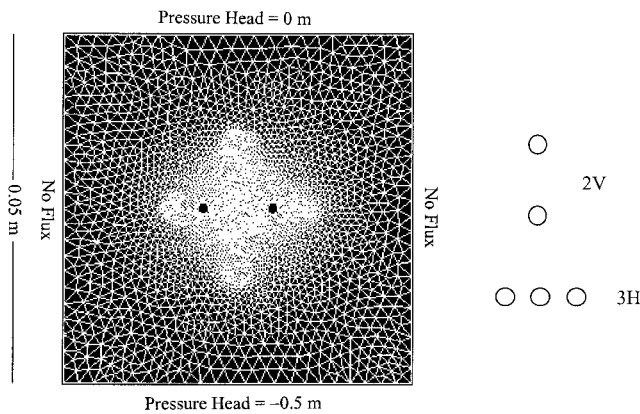
dielectric permittivity distribution in the vertical plane. Equation [1] can be rearranged to define the "measured" water content based on this dielectric permittivity. The inversion capabilities of HYDRUS-1D (Šimůnek et al., 1998) were subsequently used to determine the hydraulic parameters that best fit the 26 probe-measured water contents as a function of time. HYDRUS-1D uses the Levenberg–Marquardt optimization technique to minimize the sum of squared deviations of measured and computed variables. The soil hydraulic properties were defined using the van Genuchten (1980) formulations. The Brooks and Corey (1964) formulations, or a step function, could have been used to examine a very sharp wetting front, thereby increasing the expected errors. However, we chose to use the van Genuchten (1980) form to determine whether smoothing at a wetting front would greatly reduce errors due to TDR spatial sensitivity. For the inversion, the saturated water content, θ_s, the residual water content, θ_r, and the l parameter (Mualem, 1976) were held constant with values of 0.43, 0.045, and 0.5, respectively. These values are equal to those used for the forward flow simulations with HYDRUS-2D. The inversion optimized the values of the van Genuchten parameters α (m^{-1}) and n, and the saturated hydraulic conductivity, K (m s^{-1}) for the relationships:

$$\theta = \theta_r + \frac{\theta_s - \theta_r}{(1 + |\alpha h|^n)^m} \text{ for } h < h_s, \text{ and}$$

$$\theta = \theta_s \text{ for } h \geq h_s \qquad [2]$$

$$Se = \frac{\theta - \theta_r}{\theta_s - \theta_r} \qquad [3]$$

$$K(h) = K_s Se^{0.5}[1 - (1 - Se^{1/m})^m]^2 \qquad [4]$$

where h is the pressure head (m) and h_s is the air-entry value. The value of each of the fitted parameters that was used in the forward flow model was used as an initial guess for the inversion.

RESULTS

Limitations of One-Dimensional Inversion of Wetting Front Data

One objective of this investigation was to determine the impacts of the distributed spatial sensitivity of TDR on the monitoring of wetting fronts. Specifically, we investigated the inversion of hydraulic parameters from water content measurements collected during the advance of a wetting front. However, it should be recognized that, in general, inverse modeling does not necessarily guarantee unique values of inverted properties. Furthermore, the forward flow model used in these analyses (HYDRUS-2D) was not identical to the inverse model used (HYDRUS-1D). For example, HYDRUS-2D uses the finite element method for a spatial discretization of the Richards equation, while HYDRUS-1D uses finite differences. Therefore, we conducted an initial numerical experiment to identify errors and uncertainties associated with the inverse modeling of a wetting front given exact knowledge of the water content at a single observation point. An equally weighted 26-point objective function was formed from the water content time series at the observation node with no rods present (all circles filled with elements). The correct soil hydraulic

properties were used as initial estimates in the inverse model. Thus, the objective of this study was not to determine the uniqueness of optimized parameters, but, rather, to determine how much information is lost when TDR-measured water contents are used to form the objective function. Finally, similar spatial discretization was used in both the HYDRUS-1D and HYDRUS-2D models, with the nodal spacing of 0.05 cm for HYDRUS-1D and an average nodal spacing of 0.08 cm for HYDRUS-2D with higher resolution near the rods. The time discretization, initial conditions, and boundary conditions were identical in both models.

The observed and fitted water content time series (Fig. 2) showed excellent agreement ($R^2 = 0.99998$), suggesting that there is very little error introduced by the combined use of HYDRUS-2D for forward modeling and HYDRUS-1D for inversion. (Note that the observations are based on the actual water content at the midpoint of the domain, not on the TDR-measured water content time series.) The fitted values of α, n, and K_s are shown in Table 1 and are referred to as the "No rods" scenario. The inverted values were used to construct characteristic curves (Fig. 3). The actual soil characteristic curves (thick lines) and the no rod inversion (thin lines) are virtually identical. Furthermore, the 95% confidence intervals for the inverted parameters are very narrowly defined (Table 1). Confidence intervals of optimized parameters are calculated in HYDRUS-1D from knowledge of the shape of the objective function at its minimum, the number of observations, and the number of unknown fitted parameters. It is desirable that the estimated mean value be located in a narrow interval. Large confidence limits indicate that the results are not very sensitive to the value of a particular parameter. Given that the confidence intervals will be a function of the exact choice of parameters to fit, the reported values should not be taken to describe the absolute accuracy of the inversion of hydraulic parameters from TDR measurements. Rather, the relative values of the confidence intervals should be used to compare the suitability of several probe designs. The region between the dashed lines on Fig. 3 shows the full range of values
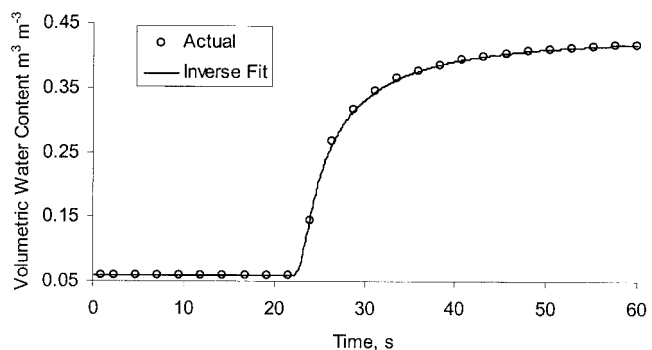

Fig. 2. The water content breakthrough curve at the midpoint of the domain with no rods present determined through forward modeling with HYDRUS-2D (Actual) and the water content breakthrough curve predicted (Fitted) based on optimized values for the saturated hydraulic conductivity and van Genuchten's (1980) α and n parameters as determined by numerical inversion of the observed water contents with HYDRUS-1D.
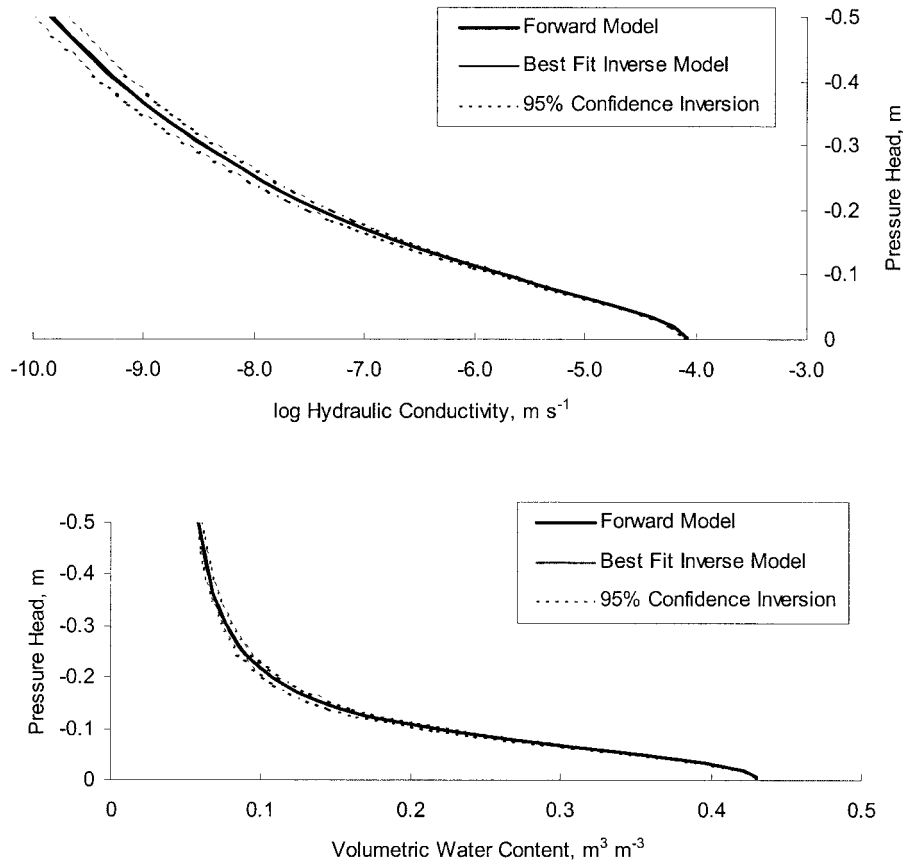
Fig. 3. The inverted soil hydraulic functions based on optimization of the actual water content at the center of the two-dimensional domain with no rods present lie within a very narrow range (region between the dashed lines) that includes the correct functions (thick lines). The fitted functions (thin lines) produce an excellent estimate of the correct functions.

describing the characteristic curves that lie between curves calculated with the 95% confidence intervals of the inverted van Genuchten (1980) parameters. The uppermost dashed line was formed using the highest values of α, n, and K_s within the 95% confidence interval, and the lowermost line used the lowest values.

Effects of TDR Rods on Wetting Front Advance

The water content time series at the center of the domain with no rods present is shown as a thick line in Fig. 4. The water content time series at the center of the domain with different 2H and 2V probes are shown to demonstrate the influence of the TDR rods on water movement at the center of the domain. Most of the probes have little observable effect on the water content breakthrough curve. A narrowly spaced 2H probe causes slightly faster breakthrough because of acceleration of the water between the rods. As would be expected from their similar geometries, a 3H probe (not shown) has an identical response as a 2H probe with one-half the outermost rod spacing; for example, a 3H(0.01) probe has the same effect as a 2H(0.005) probe. A narrowly spaced 2V probe causes a slight delay in wetting front arrival due to "shadowing" of the probe midpoint by the upper rod. Probes with larger rod separations show a much smaller effect on water movement at the probe midpoint.

The hydraulic function determined from the 2H(0.005) water content breakthrough curve is shown in Fig. 5, and the inversion results are included in Table 1. The impacts of the rods on the wetting front have little effect on the best-fit interpreted hydraulic functions, which still show excellent agreement with the actual values. The only observable effect is an increase in the width of the 95% confidence envelope, with the results of the 2H probe slightly better than those of the 2V(0.005) probe (results not shown).

The TDR-Measured Wetting Front Advance

The TDR-measured water content at any given time will be a function of the specific water content distribution around the rods at that time. Nissen et al. (unpublished data) found that the numerical approach of Knight et al. (1997) could be used to describe the spatial sensitivity of TDR probes in the presence of sharp dielectric boundaries. To better test the applicability of the numerical model of TDR sensitivity, they examined the response of probes near fluid–fluid interfaces. In this investigation, we applied this numerical analysis to include the effects of TDR rods on the distribution of water in a soil, as discussed above. The simulated responses of four TDR probe configurations are compared with the actual water content at the center of the domain with no rods present in Fig. 6. Three of the
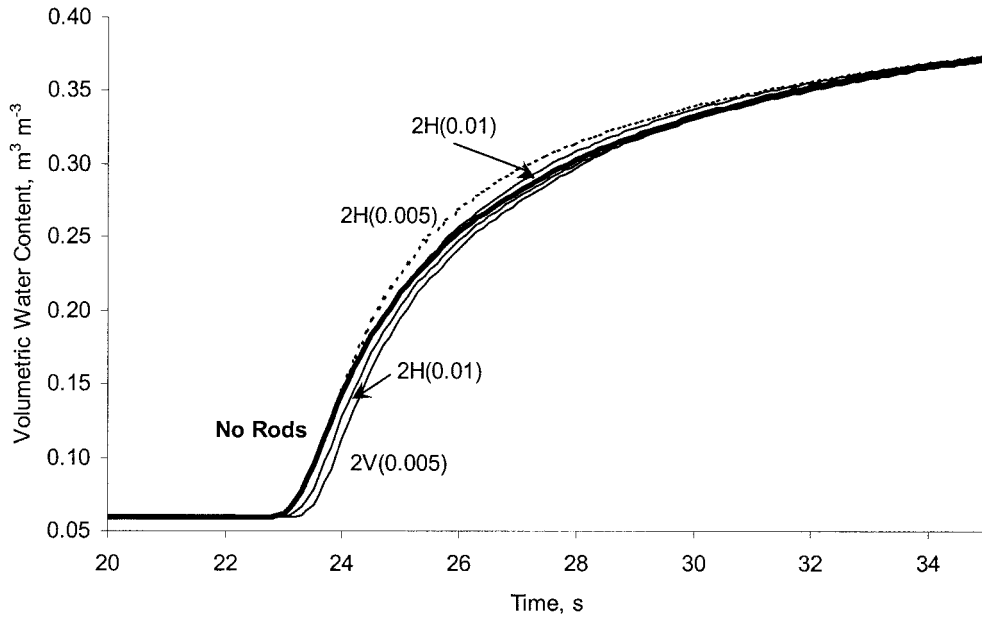
Fig. 4. Water content breakthrough curves at the mid-depth of the simulation domain with no TDR rods present and with 2H or 2V probes of varying rod separations.
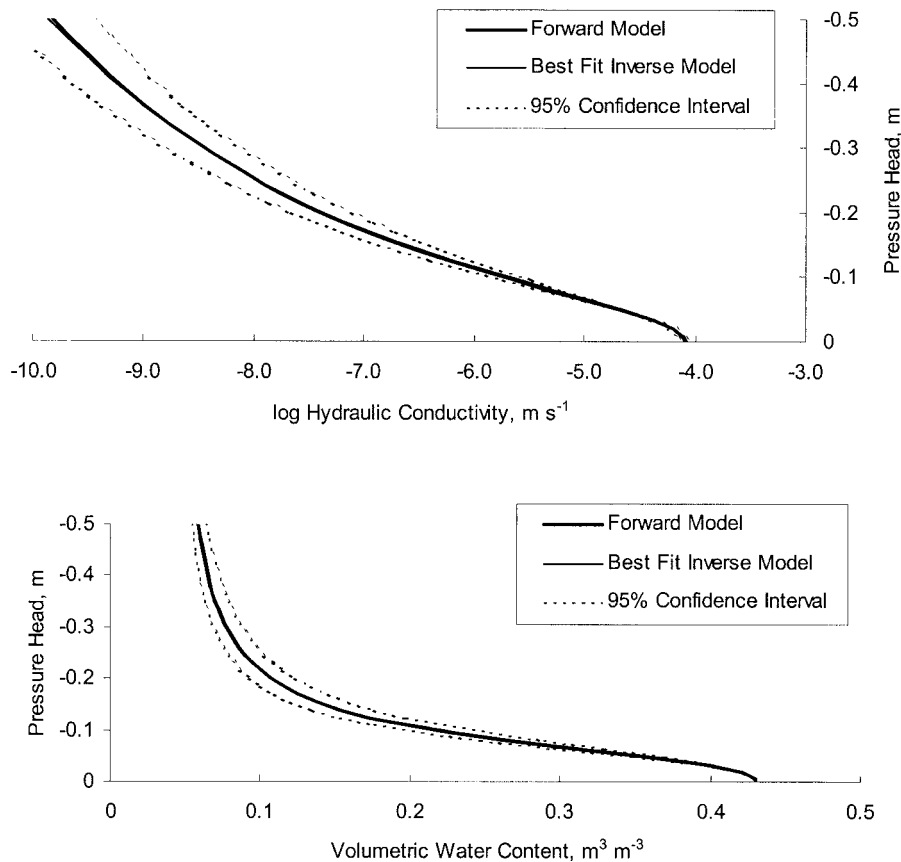

Fig. 5. The inverted soil hydraulic functions based on optimization of the actual water content at the center of the two-dimensional domain with a 2H(0.005) probe present lie within a narrow range (region between the dashed lines) that includes the correct functions (thick lines). The fitted functions (thin lines) produce an excellent estimate of the correct functions.

probes have identical rod diameters and outer rod separations. The fourth probe, 2H(0.005), is included for direct comparison with the 3H(0.01) probe. The 2V probe shows a markedly different response than the 2H or 3H probes. This probe shows an early first arrival of water and the most dramatic delay in the arrival of the wetting front (defined here as the time to reach one-half of the final water content change, shown as a horizontal
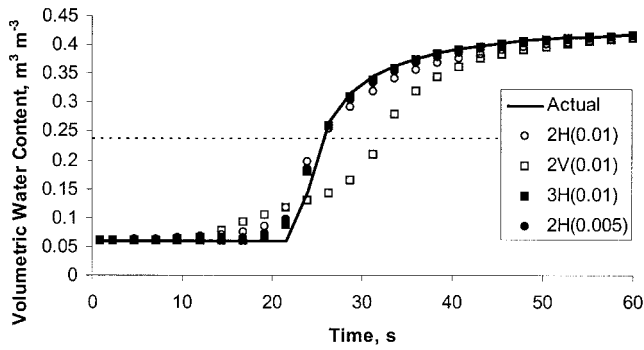
Fig. 6. Simulated TDR probe responses compared with the actual water content breakthrough curve at the center of the domain during the advance of a wetting front without rods present. The time of arrival of the wetting front is identified as the time required to reach one-half of the total water content change, which is shown as the intersection of the horizontal dashed line with each breakthrough curve.

dashed line). All of the 2H and 3H probe responses show the same time of arrival of the wetting front. A 3H probe with the same outer rod separation shows less effect of spatially distributed sensitivity than a 2H probe with the same separation. However, the response of a 3H probe and a 2H probe with the same distance between adjacent rods is very similar [i.e., 3H(0.01) vs. 2H(0.005) probes].

The TDR responses can be explained based on an understanding of the sample areas of TDR probes (Ferré et al., 1998; Nissen et al., unpublished data). Specifically, 3H probes have very restricted sample areas, with the probe sensitivity concentrated in the region immediately adjacent to the central rod. In contrast, a 2H probe with the same outer rod separation has a sample area that is more evenly distributed in an approximately elliptical region surrounding the probe rods. In a homogeneous medium, a 2V probe has a sample area that is identical to that of a 2H probe of the same dimensions, rotated by 90°. However, Nissen et al. (unpublished data) found that if the dielectric permittivity varies between the rods, the sample area of a 2V probe is strongly biased toward the region of lower dielectric permittivity. This bias arises because all of the energy must flow through both the high and low dielectric permittivity regions, but the potential gradient is much higher through the low dielectric permittivity region than through the high dielectric permittivity region. Given that the energy can be defined based on the square of the gradient of the potential, the energy, and therefore the probe sensitivity, is concentrated within the low dielectric permittivity region. One result of this is that while horizontal probes will measure the arithmetic average of the dielectric permittivities ahead of and behind a sharp wetting front that intersects the probe midpoint, a vertical probe will measure the harmonic mean dielectric permittivity (Ferré et al., 1996). As a result, 2V probes will overweight the dry region between the wetting front and the lower rod, giving a lower water content when the wetting front is located between the rods. On the basis of their sample areas, it is expected that the 3H probe will preserve more of the sharpness of the wetting front in the water

content breakthrough curve than will a 2H with the same outer rod separation. Furthermore, horizontal probes are expected to show the correct time of arrival of a step function wetting front. The modeling results demonstrate that this result extends to a more dispersed wetting front as well. Meanwhile, the 2V probe will sense the arrival of the wetting front before the wetting front reaches the probe midpoint because the upper rod is located above the probe midpoint. Then, the changing spatial sensitivity of the 2V probe with further advance of the wetting front gives rise to a complex water content breakthrough curve. Nissen et al. (unpublished data) found that a 2V probe does not sense a sharp dielectric permittivity boundary until both rods are in contact with the higher dielectric permittivity region. This may suggest that the inversion of the 2V results could be improved by considering the measurement point to be located at the center of the lowest rod. In fact, the shape of the wetting front is so badly distorted by this probe configuration that this approach gives only marginally better inversion results (not shown).

Hydraulic Properties Determined from TDR-Measured Water Contents

The spatially distributed sensitivity of TDR probes has a clear effect on the shape of water content breakthrough curves. Therefore, researchers must be cautious when making detailed interpretations of water breakthrough curves based on TDR measurements. This caution also applies to measurements made with other instruments that have spatially distributed sensitivities. However, it is unclear from direct observation of the water content breakthrough curves how the distortion of the wetting front shape will impact the interpretation of basic hydraulic properties derived assuming point water content measurements. To examine this, HYDRUS-1D was used to infer the values of α, n, and K_s from the simulated probe responses for the 2V(0.01), 2H(0.01), 3H(0.01), and 2H(0.005) probes. The fitted values and the 95% confidence interval of the parameter values are shown in Table 1. The best-fit inverse models show good agreement with the simulated TDR-measured water breakthrough curves, giving R^2 values in excess of 0.96 for all probes. The 3H probe shows the smallest range between the upper and lower 95% confidence intervals for all of the estimated values. Even comparing the 2H(0.005) and 3H(0.01) probes shows that although these probes had nearly identical actual water content breakthrough curves at the probe midpoints, the larger sampling area of the 2H probe led to slightly greater smoothing of the water content breakthrough curve. This leads to less accurate hydraulic property inversions.

The interpreted water retention and hydraulic conductivity functions are shown in Fig. 7 and 8 for the modeled TDR probes. As in Fig. 3, the region between the dashed lines shows the range of hydraulic functions that lie within the 95% confidence interval of the inversion. The accuracy of the fit is much better and the width of the 95% confidence interval is much narrower
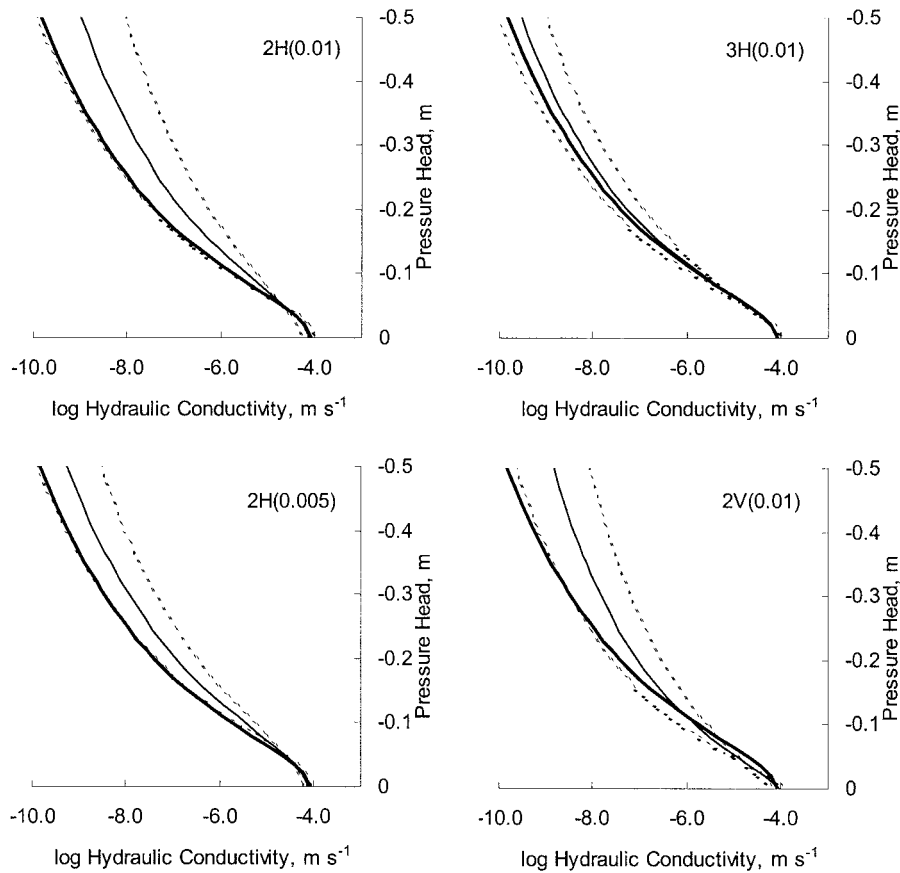
Fig. 7. Fitted log hydraulic conductivity based on water content observations made with 2H(0.01), 3H(0.01), 2V(0.01), and 2H(0.005) probes. The thick lines show the soil parameters used in the forward model. The region between the dashed lines on each panel shows the 95% confidence interval. The thin lines show the best-fit parameters.

Fig. 8. Fitted hydraulic functions based on water content observations made with 2H(0.01), 3H(0.01), 2V(0.01), and 2H(0.005) probes. The thick lines show the soil parameters used in the forward model. The region between the dashed lines on each panel shows the 95% confidence interval. The thin lines show the best-fit parameters.
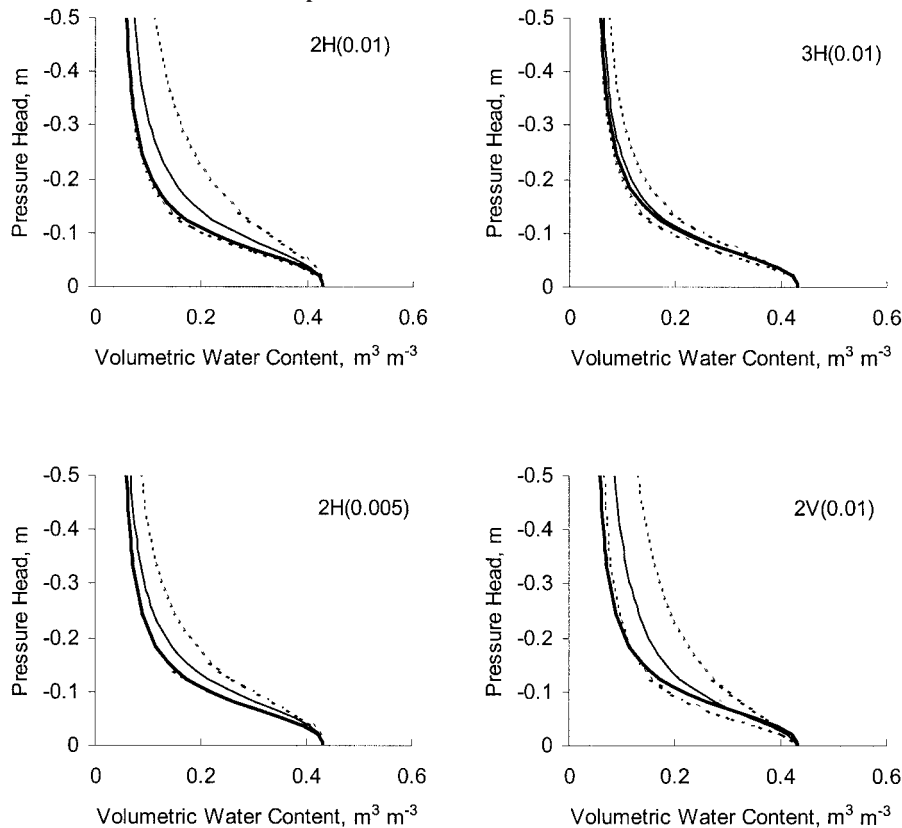
for the inversion based on the water content at the midpoint of a domain including a 2H(0.005) probe (Fig. 3) than for the inversion based on the TDR-measured water contents for this case (Fig. 7 and 8). Similar comparisons can be made for the 2H(0.01), 2V(0.01), and 3H(0.01) probes based on the results reported in Table 1. These results demonstrate the direct impact of the spatial sensitivity of TDR on hydraulic property inversions. That is, for the relatively thin rods examined, we can conclude that the effects of flow disturbance by the probes is insignificant compared with the effects of the spatially distributed sensitivity of TDR. The uncertainty introduced into the inversion of hydraulic parameters because of the spatial averaging of TDR probes is minimized by the use of 3H probes. Furthermore, the predicted hydraulic properties based on measurements made with 3H probes agree most closely with the correct values. Compared with the 3H responses, equally sized 2H and 2V probes lead to unacceptably uncertain parameter estimates. For the 2V probe, the correct hydraulic conductivity function lies outside of the 95% confidence interval at low water pressures. As a result, this configuration is not recommended for monitoring the advance of a wetting front.

CONCLUSIONS

Numerical analysis of the response of TDR probes to the advance of a wetting front shows that the distributed spatial sensitivity of TDR probes leads to smoothing of the observed wetting front. The observed wetting front shape is more distorted for vertically emplaced probes than for horizontal probes. The distortion caused by horizontal probes decreases with a decrease in the rod separation. However, with decreases in the rod separation, the impact of the rods on the flow of water increases. In practice, this effect can be reduced by the choice of relatively small TDR rods. The optimal TDR probe configuration for inversion of hydraulic parameters from wetting front monitoring was a narrowly spaced 3H design. Despite the effects of this probe on water flow, the highly concentrated spatial sensitivity of this probe leads to minimal smoothing of the water content breakthrough curve. This result suggests that 3H probes with a very small rod separation will capture the water content breakthrough curve most accurately, leading to optimal hydraulic parameter inversion. However, this conclusion must be balanced by the tendency of probes with very small rod spacings to be highly sensitive to the effects of disturbance during insertion of rods into the medium or during packing of the medium around the rods. Given this practical concern, we recommend that a larger separation, on the order of five times the rod diameter, be used with 3H probes to monitor the

advance of a wetting front. This specific recommendation for the application of TDR monitoring to wetting fronts cannot be adopted generally for all monitoring applications. Rather, we recommend that a similar analysis be performed for each specific monitoring application. Direct examination is especially warranted for probes with components that would be expected to produce more disturbance to flow (e.g., rods mounted on substrates) or rods with shapes that may lead to nonuniform concentration of probe sensitivity (e.g., flat plates with sharp corners). In theory, the method of analysis presented could also be used to examine the response of very thin rods, with diameters approaching the grain size of the surrounding material. However, this will require a more accurate representation of the distributions of grains, water movement, and variations in the dielectric permittivity of pore water at such small scales. Finally, while the results shown here are specific to TDR responses, the same consideration should be given to all instruments with spatially distributed sensitivities.

REFERENCES

Brooks, R.H., and A.T. Corey. 1964. Hydraulic properties of porous media. Hydrology Papers. Colorado State University, Fort Collins, CO.

Ferré, P.A., J.H. Knight, D.L. Rudolph, and R.G. Kachanoski. 1998. The sample area of conventional and alternative time domain reflectometry probes. Water Resour. Res. 34:2971–2979.

Ferré, P.A., D.L. Rudolph, and R.G. Kachanoski. 1996. Spatial averaging of water content by time domain reflectometry: Implications for twin rod probes with and without dielectric coatings. Water Resour. Res. 32:271–279.

Knight, J.H. 1992. Sensitivity of time domain reflectometry measurements to lateral variations in soil water content. Water Resour. Res. 28:2345–2352.

Knight, J.H., P.A. Ferré, D.L. Rudolph, and R.G. Kachanoski. 1997. The response of a time domain reflectometry probe with fluid-filled gaps around the rods. Water Resour. Res. 33:1455–1460.

Mualem, Y. 1976. A new model for predicting the hydraulic conductivity of unsaturated porous media. Water Resour. Res. 12:513–522.

Nissen, H.H., P.A. Ferré, and P. Moldrup. 2002. Metal-coated printed circuit board time domain reflectometry probes for measuring water and solute transport in soil. Water Resour. Res. In press.

Schaap, M.G., F.J. Leij, and M.Th. van Genuchten. 2001. Rosetta: A computer program for estimating soil hydraulic parameters with hierarchical pedotransfer functions. J. Hydrol. 251:163–176.

Šimůnek, J., M. Šejna, and M.Th. van Genuchten. 1998. The HYDRUS-1D software package for simulating the one-dimensional movement of water, heat, and multiple solutes in variably-saturated media. Version 2.0, IGWMC-TPS-70. International Ground Water Modeling Center, Colorado School of Mines, Golden, CO.

Šimůnek, J., M. Šejna, and M.Th. van Genuchten. 1999. The HYDRUS-2D software package for simulating two-dimensional movement of water, heat, and multiple solutes in variably saturated media. Version 2.0, IGWMC-TPS-53. International Ground Water Modeling Center, Colorado School of Mines, Golden, CO.

Topp, G.C., J.L. Davis, and A.P. Annan. 1980. Electromagnetic determination of soil water content: measurement in coaxial transmission lines. Water Resour. Res. 16:574–582.

van Genuchten, M.Th. 1980. A closed-form equation for predicting the hydraulic conductivity of unsaturated soils. Soil Sci. Soc. Am. J. 44:892–898.